Miniband transport in vertical superlattice field-effect transistors

R. A. Deutschmann,[a] W. Wegscheider,[b] M. Rother, M. Bichler, and G. Abstreiter
Walter Schottky Institut, TU München, Am Coulombwall, 85748 Garching, Germany

(Received for publication 16 February 2001; accepted for publication 5 June 2001)

We study the nonequilibrium transport of two-dimensional electrons through a periodic potential. Our samples are fabricated using the cleaved-edge overgrowth technique to provide a vertical field-effect transistor with an undoped GaAs/AlGaAs superlattice channel orthogonal to the current flow. We find a pronounced negative differential resistance, the magnitude of which increases with increasing modulation strength. The data are qualitatively consistent with the Esaki–Tsu transport model in minibands, which we calculate for the given samples. We emphasize the significance of the two-dimensionality of the electron system and the gate to inhibit domain formation. Weak features in the source-drain current are attributed to Bloch-phonon resonances. © *2001 American Institute of Physics.* [DOI: 10.1063/1.1390320]

It has long been a dream to fabricate the Bloch oscillator: an electronic device that emits tunable high frequency radiation upon application of a dc voltage. In a simple physical picture electrons are accelerated by the electric field, and oscillate in real and reciprocal space due to Bragg reflections at the Brillouin zone boundary. The existence of Bloch oscillations (BOs) has indeed been proven by laser excitation of Wannier–Stark states[1] in semiconductor superlattices[2] (SLs). However, the more practicable concept of electrical excitation suffers from the tradeoff between high current (high doping level) and long scattering time (low doping level). Additionally, in bulk superlattices at the presence of a local negative differential resistance (NDR) the charge distribution becomes unstable and causes low-field and high-field domains, disrupting the BOs. Here we present a device structure which improves on these issues. First, in our vertical field-effect transistor high electron densities can be set simply by the gate without the need for any doping. Second, the reduced dimensionality of the electron system with respect to bulk SLs and the presence of a metallic gate in close vicinity serve to stabilize the charge distribution in the SL even in the regime of NDR.

Sakaki *et al.*[3] theoretically consider a modulated two-dimensional electron gas (2DEG) by extending previous theoretical work on electron transport in bulk SLs at finite Fermi energy.[4] Stiles[5] discusses possible three terminal field-effect devices, which have subsequently been realized on vicinal surfaces[6] and using grid metallic gates.[7,8] The vicinal surface devices, relying on self-organization, hardly achieve regular potential modulations, while the grid gate devices, although well defined, are limited to period lengths above ~100 nm and weak potential modulations due to the distance between the surface gates and the 2DEG.

Our design, using the cleaved-edge overgrowth technique,[9] overcomes these limitations because atomically precise potential modulations with freely adjustable amplitudes are readily achieved. As shown in Fig. 2(c), in a first MBE growth step an undoped SL of N periods 12 nm GaAs/3 nm $Al_{0.3}Ga_{0.7}As$ (period length $a = 15$ nm) is grown between two n^+ GaAs contacts (source and drain) on semi-insulating (001) GaAs. After *in situ* cleavage, a second growth step of d nm GaAs, 100 nm AlAs, and 200 nm n^+ GaAs gate follows on the freshly exposed (110) surface. By positively biasing the gate with respect to source and drain (gate voltage $U_g = 0-1$ V) a two-dimensional electron gas (2DEG) of density $n_s = 0-6\times10^{11}\ \mathrm{cm}^{-2}$ is induced. Our superlattice field-effect transistor (SLFET) differs from the original device invented by Stormer *et al.*[10] in three important ways. First we use n^+ GaAs source and drain contacts instead of n^+ SL contacts, which is crucial to avoid leakage currents through the bulk SL at finite source-drain bias. Second we use an n^+ GaAs gate instead of a fixed doping to obtain tunable electron density and higher electron mobility due to the absence of remote ionized impurity scattering. Third a new degree of band structure design is added since by proper choice of the GaAs (110) layer thickness d the strength of the potential modulation can be tuned without changing the SL. Previously only devices with $d = 0$ nm have been investigated in magnetotransport[11,12] and nonequilibrium transport.[13,14] Recently, magnetotransport studies of long-period SLFETs have revealed clear band-structure effects.[15] Here we systematically investigate short-period SLFETs with $(N,d) = (100,\ 0\ \mathrm{nm})$, (200, 4 nm), (200, 10 nm), and (200, 20 nm) and reference FETs where the SL was replaced with a homogenous $Al_{0.067}Ga_{0.933}As$ layer (the chosen Al content matches the mean Al content in the SL). All measurements are performed at 1 K in liquid He, the drain voltage is applied to the top n^+ layer, two voltage probes detect the actual voltage drop across the 2DEG.

A series of $I-V$ measurements is shown in Fig. 1 for all four SLFETs. For a gate voltage $U_g = 0$ V the source-drain current I_{sd} is smaller than 1 μA for all samples. Above $U_g = 0.13$, 0.11, 0.06, and 0.02 V, respectively, I_{sd} saturates at a finite current. For slightly larger gate voltages current saturation is preceded by a NDR for $U_{sd} > 25$, 35, 45, and 50 mV, respectively. In addition, the strength of the NDR decreases with increasing thickness d, but NDR is found even in the sample with $d = 20$ nm. The saturation currents are larger for

[a]Electronic mail: deutschmann@wsi.tum.de
[b]Present address: Universität Regensburg, Universitätsstr. 31, 93040 Regensburg, Germany.

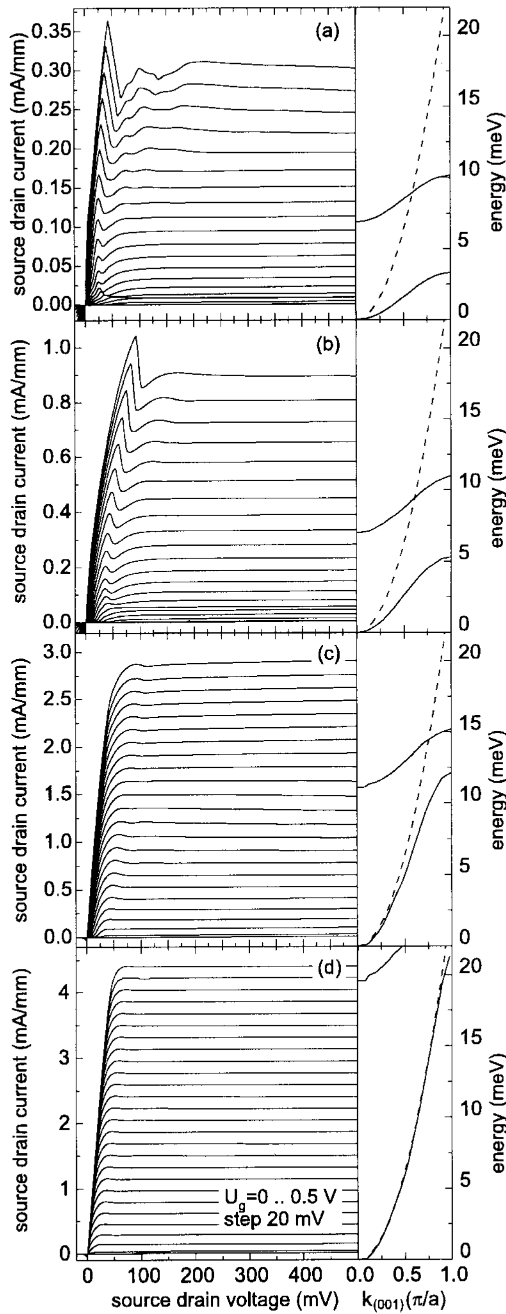

FIG. 1. Current–voltage characteristics and calculated band structure of the two lowest minibands for the different SLFETs (dotted: free electron dispersion). (a) $d=0$ nm, $\Delta_1=3.3$ meV, $\Delta_2=3.3$ meV; (b) $d=4$ nm, $\Delta_1=5.3$ meV, $\Delta_2=3.8$ meV; (c) $d=10$ nm, $\Delta_1=12.2$ meV, $\Delta_2=3.8$ meV; (d) $d=20$ nm, $\Delta_1=21.2$ meV, $\Delta_2=5.0$ meV.

larger d. The reference samples show normal FET behavior with comparable saturation currents to the SLFETs, but no NDR.

The influence of d on the band structure in the SLFETs is revealed by self-consistent two-dimensional quantum mechanical calculations, as shown in Fig. 1 next to the respective SLFET traces. For $d=0$ nm the miniband width $\Delta_1=3.3$ meV. The second miniband of width $\Delta_2=3.3$ meV originates from excited states in the (110) direction, and is offset from the first miniband by the (110) quantization energy.[16] We note that Δ_1 and Δ_2 only weakly depend on the electron density, and are separated by a minigap. For $d=0$ nm magnetotransport experiments and calculations using the known density of states have shown[11,13] that the Fermi energy E_F reaches Δ_1 for $U_g=0.4$ V. For increasing d Δ_1 also increases, indicating the weaker influence of the SL on the electron gas. Δ_2 remains almost unchanged, because the corresponding electron states are located in the SL. For $d \geqslant 10$ nm both minibands even overlap, and for $d=20$ nm the electron dispersion is almost equal to that of the free electron.

We interpret the SLFET data in terms of Esaki–Tsu type miniband transport under the assumption of constant electric field across the SL. Electrons are accelerated towards the Brillouin zone boundary, and, unless scattered, are Bragg reflected, which results in electron localization and a decreasing current. Calculations[3,4] have shown that (I) even when $E_F>\Delta$ for 2D electrons the current and NDR persists, unlike the 1D case, where the current is expected to quench at filled bands (II) the position of the NDR depends on the scattering time and is not directly dependent on E_F (III) the peak current increases with increasing Δ. These findings are in qualitative agreement with our data, but it must be noted that they are based on the assumption of a constant relaxation time and sinusoidal energy band, which need to be relaxed for quantitative agreement.

Further experimental evidence for Esaki–Tsu type miniband transport is obtained by comparing the electron *quantum* mobility $\mu_Q=B_c^{-1}$, obtained from the onset of Shubnikov–de Haas oscillations at the magnetic field B_c with the Esaki–Tsu mobility $\mu_{ET}=\Delta dL/2\hbar U_p$, related to the peak voltage U_p(L=channel length). For all samples we find good agreement between these mobilities, e.g., for the SLFET with $d=0$ nm $\mu_Q \cong \mu_{ET} \cong 3\times10^4$ cm^2/V s, and for $d=20$ nm $\mu_Q \cong \mu_{ET} \cong 1.2\times10^5$ cm^2/V s. This remarkable fact indicates that relevant scattering events for BOs are the ones that are phase breaking with phase coherence time $\tau \propto \mu_Q$, μ_{ET}.

In the following we rule out other possible reasons besides Bloch localization that could theoretically lead to NDR. (I) *Intersubband scattering* might occur since U_p is comparable to the subband separation, and for $d>10$ nm the subbands even overlap. For $d>0$ nm Δ_2 is always smaller than Δ_1 and due to the heavier electron mass in the upper band, NDR could be expected. However, this rationale is not applicable to the $d=0$ nm case, where both subbands have the same width and mass, and the mobility in the higher subband will even be larger due to the larger distance of the electrons from the interface. Therefore the NDR of this sample cannot be explained by intersubband scattering. Additionally, the strength of the NDR decreases with increasing d, even though the difference in effective mass of both subbands increases, which also rules out such an explanation for the NDR. (II) *Intervalley scattering* can be excluded because the energy separation between the Γ and L minima in GaAs is much larger than the energy even of ballistic electrons at U_p. (III) *Real space transfer* across the gate barrier can be ruled out because the gate current is orders of magnitude smaller than the source-drain current. (IV) *Breakdown of the electric field* in NDR devices into high- and low-field domains may be a major obstacle for operating bulk SL devices beyond U_p. In our SLFETs, however, no sudden jumps in the current at voltages $U_{sd}>U_p$ are observed. Additionally both

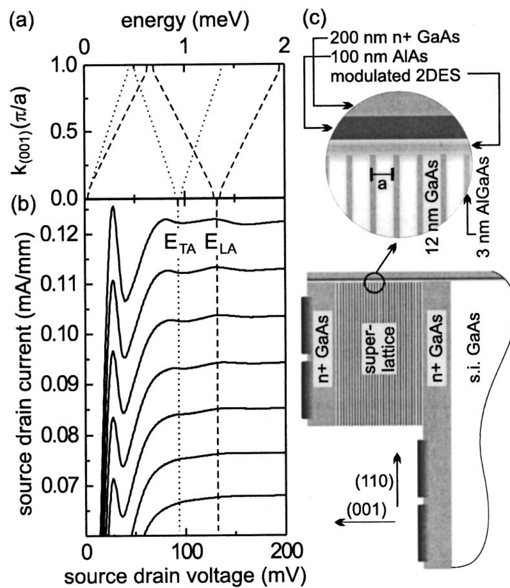

FIG. 2. (a) Acoustic phonon dispersion relation (dotted: TA, $v=3.4\times10^3$ m/s; dashed: LA, $v=4.8\times10^3$ m/s) calculated using the respective sound velocities v, minigaps schematically drawn (b) enlargement of the $d=0$ nm SLFET $I-V$ curve of Fig. 1 for $U_g=0.27-0.33$ V (c) SLFET sample design.

sweep directions yield identical traces (no hysteresis), almost identical traces are also obtained for both current directions and even from different samples. Sudden jumps observed only at high current levels in the $d=0$ and $d=4$ nm SLFETs are solely due to the external load resistance. We are therefore certain that no sudden breakdown of the electric field occurs in our SLFETs. The charge distribution in our devices is stabilized even at the presence of NDR because of two reasons, both related to screening. First, in a 2DEG a possible charge accumulation is one dimensional, and its resulting electric field decays inversely proportional with distance, while in bulk SLs the field caused by a plane charge is independent of the distance. Second, the screening presence of a metallic gate close to the 2DEG electrostatically prevents excessive charge accumulation. (V) We can rule out NDR due to *breakdown of the miniband picture and sequential resonant tunneling* because even for the narrowest miniband width of $\Delta_1=3.3$ meV the localization length $\lambda=\Delta L/eU_p$ at the NDR is more than 13 periods of the SL.

Finally we point out a scattering mechanism to explain why the source-drain current increases again beyond the NDR peak. As shown in Fig. 2(b), weak current resonances are observed at $U_{sd}=93$ mV and $U_{sd}=132$ mV in the $d=0$ nm SLFET. Under the assumption that electrons perform Bloch oscillations, the rf energy at these voltages is $E_B=eU_{sd}d/L=0.93$ and 1.32 meV, respectively. Surprisingly, these energies are also theoretically obtained for longitudinal and transversal acoustic phonons, that are folded back to the $k=0$ momentum state at the Brillouin zone boundary $k=\pi/a$, [see Fig. 2(a)]. Folded phonons in SLs have previously been detected with Raman scattering experiments,[17] but never in transport experiments. We suggest that folded phonons are resonantly emitted when the Bloch energy matches the folded phonon energy, which lifts electron localization and results in an increased source-drain current.

In summary we introduce a vertical field-effect transistor, that allows us to investigate Esaki–Tsu miniband transport of two-dimensional electrons within, and adjacent to, atomically precise SLs, thus probing different miniband widths. Our work contributes to the quest for the electrically driven Bloch oscillator.

The authors gratefully acknowledge valuable help by M. Grayson, F. Ertl, A. Wacker, and G. Zandler and the support by the DFG via SFB 348 and the BMBF under Contract No. 01BM918.

[1] For a review on Bloch oscillations see, K. Leo, Semicond. Sci. Technol. **13**, 249 (1998).
[2] L. Esaki and R. Tsu, IBM J. Res. Dev. **14**, 61 (1970).
[3] H. Sakaki, K. Wagatsuma, J. Hamasaki, and A. Saito, Thin Solid Films **36**, 497 (1976).
[4] P. A. Lebwohl and R. Tsu, J. Appl. Phys. **41**, 2664 (1970).
[5] P. J. Stiles, Surf. Sci. **73**, 252 (1978).
[6] J. Motohisa, M. Tanaka, and H. Sakaki, Appl. Phys. Lett. **55**, 1214 (1989).
[7] G. Bernstein and G. K. Ferry, J. Vac. Sci. Technol. B **5**, 964 (1987).
[8] K. Ismail, W. Chu, D. A. Antoniadis, and H. I. Smith, Appl. Phys. Lett. **52**, 1071 (1988).
[9] L. Pfeiffer, K. W. West, H. L. Stormer, J. P. Eisenstein, K. W. Baldwin, D. Gershoni, and J. Spector, Appl. Phys. Lett. **56**, 1697 (1990).
[10] H. L. Stormer, L. N. Pfeiffer, K. W. Baldwin, K. W. West, and J. Spector, Appl. Phys. Lett. **58**, 726 (1991).
[11] R. A. Deutschmann, W. Wegscheider, M. Rother, M. Bichler, and G. Abstreiter, Physica E (Amsterdam) **7**, 294 (2000).
[12] A. Majumdar, L. P. Rokhinson, D. C. Tsui, L. N. Pfeiffer, and K. West, Appl. Phys. Lett. **76**, 3600 (2000).
[13] R. A. Deutschmann, A. Lorke, W. Wegscheider, M. Bichler, and G. Abstreiter, Physica E (Amsterdam) **6**, 561 (2000).
[14] C. Kurdak, A. Zaslavsky, D. C. Tsui, M. B. Santos, and M. Shayegan, Appl. Phys. Lett. **66**, 323 (1995).
[15] R. A. Deutschmann, W. Wegscheider, M. Rother, M. Bichler, G. Absteiter, C. Albrecht, and J. H. Smet, Phys. Rev. Lett. **86**, 1857 (2001).
[16] The second miniband associated with the (110) *ground state* has a minimum energy at $k=\pi/a$ beyond the energy scale of Fig. 1.
[17] C. Colvard, T. A. Gant, M. V. Klein, R. Merlin, R. Fischer, H. Mockoç, and A. C. Gossard, Phys. Rev. B **31**, 2080 (1985).